Article

Discovery Medicine 2025; 37(202): 2567–2578
https://doi.org/10.24976/Discov.Med.202537202.215

DNMT3B Silencing Inhibits Malignant Phenotype of Breast Cancer by Suppressing FBXO31 Methylation

Jun Li[1], Shan Huang[1], Zhun Zhang[1], Lei Cai[1], Yanguang Wen[1,*]

[1]Department of Breast and Thyroid Surgery, The Third Xiangya Hospital of Central South University, 410013 Changsha, Hunan, China
*Correspondence: wenyanguang9028@163.com (Yanguang Wen)
Submitted: 11 July 2025 Revised: 22 August 2025 Accepted: 24 September 2025 Published: 20 November 2025

Background: Abnormal DNA methylation has been detected in breast cancer (BC). Downregulation of F-box protein 31 (FBXO31) in BC and its upregulated methylation level have been initially confirmed via bioinformatic analyses. Likewise, DNA methyltransferase 3 beta (DNMT3B) is highly expressed in BC. Accordingly, this study is engineered to fathom out whether DNMT3B can affect the progression of BC (Luminal A type) by regulating FBXO31 methylation.

Methods: DNMT3B/FBXO31 expression and FBXO31 methylation level in BC were predicted by the University of Alabama at Birmingham Cancer Data Analysis Portal (UALCAN) database. 5-methylcytosine (5mC) site of FBXO31 was analyzed with RMBase database. After human BC cells were collected and transfected, viability, apoptosis and migration/invasion were tested by 3-(4,5-dimethylthiazol-2-yl)-2,5-diphenyl-2H-tetrazolium bromide (MTT) assay, flow cytometry, and Transwell assay, respectively. FBXO31 methylation level was determined by methylation-specific polymerase chain reaction (MSP). Expression levels of FBXO31, DNMT3B, and apoptosis/proliferation-associated proteins were evaluated using quantitative real-time reverse transcription polymerase chain reaction or Western blotting.

Results: DNMT3B expression was upregulated while FBXO31 expression was downregulated ($p = 1.62 \times 10^{-12}$), and FBXO31 methylation level was elevated in breast invasive carcinoma ($p < 1 \times 10^{-12}$). DNMT3B was highly expressed in MCF-7, MDA-MB-231 and MDA-MB-453 cells ($p < 0.001$). DNMT3B silencing inhibited viability, migration and invasion ($p < 0.05$), enhanced apoptosis ($p < 0.001$), upregulated expression levels of Bax and FBXO31 ($p < 0.001$), downregulated expression levels of B cell leukemia/lymphoma 2 (Bcl-2), Ki67 and proliferating cell nuclear antigen (PCNA) ($p < 0.001$), and diminished FBXO31 methylation level in MCF-7 cells. FBXO31 silencing showed the opposite effects in MCF-7 cells ($p < 0.001$), whereas DNMT3B silencing reversed the effects of FBXO31 silencing in MCF-7 cells ($p < 0.01$).

Conclusions: DNMT3B silencing alleviates malignant behaviors in Luminal A BC cells by suppressing FBXO31 methylation, indicating a novel mechanism of DNA methylation in Luminal A type BC.

Keywords: DNA methyltransferase 3 beta; F-box protein 31; DNA methylation modification; breast cancer; malignant phenotypes

Introduction

Breast cancer (BC) is a malignant tumor that occurs in breast epithelial cells, posing a grave threat to women [1]. Although the incidence and mortality rates of BC are relatively lower in China than in most developed countries, the continuously increasing trend has garnered mounting concerns [2]. The contributors for BC include obesity, overweight, a lack of physical activity, radiation exposure, genetic predisposition, and endogenous hormone exposure, etc. [3]. BC is classified to four molecular subtypes: Luminal A, Luminal B, Human Epidermal growth Factor receptor 2 (HER2)-positive, and triple-negative BC, with each exhibiting substantial differences in biological behaviors, treatment responses and prognosis. To date, the combination of surgery with immunotherapy and radiotherapy is a clinical therapeutic route for BC [4–6]. However, relapse and metastasis of BC remain major clinical challenges, despite considerable progress in targeted therapy, chemotherapy, and endocrine therapy, which highlight the urgency need for innovative the therapeutic strategies in the treatment of BC [7,8].

DNA methylation is an all-important part of epigenetics, playing a key role in many key processes in mammals, including ageing and carcinogenesis [9,10]. The major forms of DNA methylation consist of 5-methylcytosine (5mC), N6-methyladenine (6mA) and N4-methylcytosine (4mC) [11], which in prokaryotes and eukaryotes are responsible for promoting gene expression regulation and cellular defense [12]. Especially, accumulating evidence has demonstrated that 5mC has the ability to regulate various genes in physiological processes, and aberrant CpG island promoter 5mC can silence tumor suppressor genes and subsequently facilitate the tumor development [13]. DNA methylation can affect gene expression to mediate cancer development and progression [14]. Aberrant DNA methylation is a key factor in the development of BC [15],

which impacts the prognosis of BC through mediating gene expressions [15]. Besides, DNA methylation in the promoter region has been underlined to be negatively correlated with some gene expressions [16,17]. Therefore, identifying some key genes involved in the regulation of DNA methylation in BC is of great significance.

DNA methyltransferase 3 beta (DNMT3B), as a methyltransferase, acts on target genes to undergo methylation modifications [14]. It has been reported that DNMT3B promoter methylation is associated with cancer type, tumor size and histologic grade, suggesting that DNMT3B-promoted methylation may become a biomarker for diagnosis and prognosis of BC [18,19]. DNMT3B has been confirmed to be upregulated in BC tissues compared with normal tissues [20]. DNMT3B is involved in the maintenance of BC tumor stem cells, and is closely associated with tumor proliferation and metastasis [21]. Liu *et al*. [22] found that DNMT3B expression is higher in HER2-positive and triple-negative BC than in Luminal BC. DNMT3B overexpression enhances the proliferative, invasive, and migratory capabilities of T-47D (Luminal B type) and MDA-MB-231 (triple-negative type) cells [23]. Furthermore, DNMT3B is highly expressed in MCF-7 and ZR-75-1 (Luminal A type) cells [24]. Likewise, based on the University of Alabama at Birmingham Cancer Data Analysis Portal (UALCAN) database (https://ualcan.path.uab.edu/), we found that DNMT3B is upregulated and F-box protein 31 (FBXO31) is downregulated in breast invasive carcinoma, while FBXO31 methylation level is elevated. In BC, FBXO31 as a tumor suppressor, is lowly expressed in BC cells (such as T47D, MCF-7, MDA-MB-231, BT549, SKBR3, and BT474), and participates in regulating malignant phenotype [25]. Additionally, recent research has demonstrated that FBXO31 expression is downregulated in breast tumor cell lines and primary tumors, and its ectopic expression suppresses MCF-7 cell proliferation [26]. The presence of a 5mC site in FBXO31 has also been predicted through RMBase database (https://rna.sysu.edu.cn/rmbase/index.php). Nevertheless, whether DNMT3B can regulate FBXO31 methylation to affect the progression of BC remains poorly understood.

Collectively, this study focused on the role of DNMT3B in FBXO31 methylation in BC. Through relative cellular experiments, we confirmed that DNMT3B could downregulate FBXO31 via methylation modification, which then promotes malignant phenotype of MCF-7 cells (Luminal A type, ER+, PR+, HER2-). These findings may contribute to a deep understanding of the DNA methylation-associated mechanism in the pathogenesis of BC (Luminal A type) from a new perspective.

Materials and Methods

Bioinformatics

Data on the expression of DNMT3B and FBXO31 in breast invasive carcinoma tissues (n = 1097) and normal tissues (n = 114), as well as the FBXO31 methylation level in carcinoma (n = 793) and normal tissues (n = 97), were obtainable from the UALCAN databases (https://ualcan.path.uab.edu/). In addition, the 5mC site of FBXO31 was predicted using the RMBase database (https://rna.sysu.edu.cn/rmbase/index.php).

Cell Culture

Human BC cell lines MCF-7 (HTB-22), MDA-MB-231 (CRM-HTB-26) and MDA-MB-453 (HTB-131), along with the human normal mammary epithelial cells MCF10A (CRL-10317) were all obtained from the American Type Culture Collection (Manassas, VA, USA). All cells were cultured in Roswell Park Memorial Institute (RPMI) medium (12633012, Thermo Fisher Scientific, Waltham, MA, USA) at 37 °C with 5% CO_2. The culture medium was supplemented with 1% penicillin/streptomycin (60162ES76, Yeason, Shanghai, China) and 10% fetal bovine serum (FBS, C0235, Beyotime, Shanghai, China). All cells were authenticated by STR identification and confirmed negative for mycoplasma.

Cell Transfection

The sense oligo and antisense oligo sequences of DNMT3B/FBXO31 were inserted into a short hairpin RNA (shRNA) expression vector (ZT001, Ribobio, Guangzhou, China) to synthesize Sh-DNMT3B or Sh-FBXO31, while the corresponding negative control (Sh-NC) was also obtainable from the same source. After the cells cultured in a 96-well plate (1×10^4 cells/well) reached 90% confluence, Lipofectamine™ 3000 transfection reagent (L3000001, Thermo Fisher Scientific, USA) was applied to transfect Sh-DNMT3B or Sh-FBXO31 into MCF-7 cells. Following 48-h incubation at 37 °C, transfection efficiency was determined using quantitative real-time reverse transcription polymerase chain reaction (qRT-PCR).

The sequences involved in this part were listed as follows: Sh-DNMT3B, sense: 5′-GGTGGATTATAGACAATAA-3′, antisense, 5′-TTATTGTCTATAATCCACC-3′; Sh-FBXO31, sense: 5′-CGTTAGTTGTAGTTCTTTA-3′, antisense, 5′-TAAAGAACTACAACTAACG-3′; Sh-NC, sense: 5′-CCTAAGGTTAAGTCGCCCTCGCTC-3′, antisense, 5′- GGATTCCAATTCAGCGGGAGCGAG-3′.

Methylation-Specific Polymerase Chain Reaction (MSP)

The methylation level of FBXO31 in MCF-7 cells following the transfection with Sh-DNMT3B was evaluated by MSP assay. Genomic DNA was extracted using

the DNeasy Blood & Tissue Kit (69504, Qiagen, Hilden, Germany) and subsequently subjected to sodium bisulfite conversion with the EpiTect fast bisulfite kit (59802, Qiagen, Germany). Then, CpG islands around FBXO31 promoter region were identified using the UCSC genome browser (http://genome.ucsc.edu/). Subsequently, the FBXO31 methylation level in MCF-7 cells was quantified by SYBR Green qMSP analysis. The Qmsp reaction mixture, containing the DNA sample and a pair of specific primers, was prepared with KAPA SYBR Fast qPCR kit (07959362001, Roche, Basel, Switzerland). Amplification was performed under the following conditions: 5 min at 94 °C, 30 s at 94 °C, 30 s at 55 °C, 30 s at 72 °C for 40 cycles; 4 min at 72 °C. Finally, the PCR products were then separated by electrophoresed on 2% agarose gels (G402022, Thermo Fisher Scientific, USA) and visualized by ethidium bromide (15585011, Thermo Fisher Scientific, USA) staining under a gel imager (Chemi Doc XRS, Bio-Rad, Irvine, CA, USA). Besides, methPrimer (http://www.urogene.org/methprimer/) was applied to design two sets of qMSP primers as follows: FBXO31 (methylated): forward, 5′-ATAGTGGAGATCGATTTGAGGTATC-3′; reverse, 5′-TCCCATCTAAACCCTTACTAAACG-3′; FBXO31 (unmethylated): forward, 5′-TAGTGGAGATTGATTTGAGGTATTG-3′; reverse, 5′-TCCCATCTAAACCCTTACTAAACAC-3′. Relative methylation level of FBXO31 was calculated by $2^{-\Delta\Delta CT}$ method.

Chromatin Immunoprecipitation (ChIP)

The ChIP kit (26156, Thermo Fisher Scientific) was used for this assay. In short, MCF-7 cells were cross-linked with formaldehyde solution (F111939, Aladdin, Shanghai, China), and chromatin fragments were obtained by microbial nuclease (N128635, Aladdin, Shanghai, China) digestion. Then, the harvested chromatin sample was incubated with anti-DNMT3B (1:100, ab227883, Abcam, Cambridge, UK) or negative control IgG (1:100, ab172730, Abcam, UK) at 4 °C overnight, along with 20 µL of protein A/G agarose. Following the elution of immunoprecipitation and DNA recovery, the purified DNA was subjected to the PCR analysis.

Quantitative Real-Time Reverse Transcription Polymerase Chain Reaction (qRT-PCR)

Total RNA was isolated from BC cells using Trizol Reagent (R0016, Beyotime, China), and reversely transcribed into the first-strand complementary DNA (cDNA) using cDNA synthesis kit (#1708890, Bio-Rad, USA). Thereafter, the cDNA was subjected to qRT-PCR analysis carried out with Fast SYBR™ Green Master Mix (4385612, Thermo Fisher Scientific, USA) in AriaMx real-time PCR instrument (G8830A, Agilent, Santa Clara, CA, USA). The reaction was developed under the following conditions: at 95 °C for 2 min, followed by 40 cycles at 95 °C for 3 s, and 60 °C for 30 s. Relative gene expression was determined using the $2^{-\Delta\Delta CT}$ method [27], with glyceraldehyde-3-phosphate dehydrogenase (GAPDH) normalized as the internal references.

The primer sequences were as follows: DNMT3B: forward, 5′-CCAACAACACGCAACCAGAG-3′; reverse, 5′-CTGCCACAAGACAAACAGCC-3′. FBXO31: forward, 5′-CTCCACCAAGTGCAACCAGA-3′; reverse, 5′-CATCACAATCTCCAGGCCGT-3′. GAPDH: forward, 5′-CAGCCTCAAGATCATCAGCA-3′; reverse, 5′-TGTGGTCATGAGTCCTTCCA-3′.

3-(4,5-dimethylthiazol-2-yl)-2,5-diphenyl-2H-tetrazolium bromide (MTT) Assay

Viability of MCF-7 cells was determined by MTT assay kit (KGA311, Keygen Biotech, Nanjing, China). In detail, the pre-prepared 50 µL MTT was incubated with MCF-7 cells (1×10^4 cells/well) at 37 °C for 4 h, after which 150 µL dimethyl sulfoxide (ST038, Beyotime, China) was added into each well. Finally, optical density (OD) at 490 nm was read by an Infinite M200 microplate reader (30033109, Tecan, Männedorf, Switzerland). Relative cell viability (%) = $(OD_{Experimental} - OD_{blank})/(OD_{Control} - OD_{blank}) \times 100$.

Flow Cytometry

Annexin V-FITC Apoptosis Detection Kit (CA1020, Solarbio, Beijing, China) was employed to test MCF-7 cell apoptosis. In short, 100 µL MCF-7 cell suspension was added into 5 µL Annexin V-fluorescein isothiocyanate (V-FITC) for 5-min incubation in the dark at room temperature. Then, 5 µL propidium iodide and 400 µL phosphate buffered solution (PBS, P1022, Solarbio, China) were added into the cell suspension. BD FACSAria™ Fusion flow cytometer (657825, BD Biosicences, San Diego, CA, USA) was immediately used to detect MCF-7 cell apoptosis, followed by analysis using BD FACSDiva™ software (version 8.0, BD Biosicences, USA).

Transwell Assay

The upper Transwell chamber was pre-coated with (invasion assay) or without (migration assay) 60 µL Matrigel (356234, Solarbio, China), and 2×10^5 MCF-7 cells were resuspended in serum-free RPMI 1640 medium (100 µL) and then added into the upper Transwell chamber (8.0-µm pore size, CLS3464, Corning Life Sciences, NY, USA) at 37 °C. RPMI 1640 medium (500 µL) with 10% FBS was added into the lower chamber. After 24-h of incubation, Matrigel and the cells on the upper chamber were removed by cotton swabs. Then, the cells migrating or invading into the lower chamber were fixed by 4% paraformaldehyde for 10 min at 4 °C and stained by crystal violet (G1062, Solarbio, China) for 30 min, followed by washing with PBS. The numbers of migratory and invasive cells were counted un-

der a Leica DM4 P microscope (15700129, Leica Microsystems, Wetzlar, Germany) at ×250 magnification. Relative migration rate (%) = (Number of migrating cells in the treatment group/Number of migrating cells in the control group) × 100; Relative invasion rate (%) = (Number of invasive cells in the treatment group/Number of invasive cells in the control group) × 100.

Western Blotting

The total protein was isolated from MCF-7 cells with RIPA Lysis Buffer (E-BC-R327, Elabscience, Wuhan, China), the concentration of which was determined using bicinchoninic acid (BCA) protein assay kit (C503021, Sangon Biotech, Shanghai, China). After that, the protein samples were separated by 6–12% sodium dodecyl sulfate polyacrylamide gel electrophoresis (SDS-PAGE) gels (P0012A, Beyotime, China), and transferred onto polyvinylidene fluoride (PVDF) membranes (F619536, Sangon Biotech, China). The membranes were blocked with 5% non-fat skim milk (D8340, Solarbio, China) diluted in Tris Buffered Saline with Tween-20 (TBST, T1085, Solarbio, China) for 2 h at room temperature, and incubated with following primary (4 °C, overnight) and secondary (1 h, room temperature) antibodies: DNMT3B (1:100, ab2851, 97 kDa, Abcam, UK), FBXO31 (1:1000, ab86137, 61 kDa, Abcam, UK), BCL2 associated X (Bax) (1:1000, ab32503, 21 kDa, Abcam, UK), B cell leukemia/lymphoma 2 (Bcl-2) (1:1000, ab32124, 26 kDa, Abcam, UK), Ki67 (1:100, ab16667, 358 kDa, Abcam, UK), proliferating cell nuclear antigen (PCNA) (1:1000, ab29, 29 kDa, Abcam, UK), and GAPDH (1:1000, ab8245, 37 kDa, Abcam, UK); horseradish peroxidase (HRP) labeled anti-Rabbit IgG (1:1000, ab99697, Abcam, UK) and anti-Mouse IgG (1:2000, ab6728, Abcam, UK).

Finally, the proteins were detected using the Super Signal West Dura Extended Duration Substrate (34076, Thermo Fisher Scientific, USA) and imaged with the Odyssey CLx infrared imaging system (LI-COR Biosciences, Lincoln, NE, USA). Relative protein expression level = the gray value of target protein/internal reference protein. GAPDH was used as the internal reference protein.

Statistical Analyses

GraphPad Prism 8.0 statistical software (GraphPad Software Inc., San Diego, CA, USA) was used for data analysis. Measurement data were expressed as mean ± standard deviation. The comparison of the data in this study was performed using one-way analysis of variance, followed by Tukey's post hoc test. The data were statistically significant when the p-value was below the threshold of 0.05.

Results

DNMT3B Expression was Upregulated While FBXO31 Expression was Downregulated, and Methylation Level of FBXO31 was Elevated in BC

We found that DNMT3B expression was higher (Fig. 1A, $p = 1.62 \times 10^{-12}$) while FBXO31 expression was lower (Fig. 1B, $p = 1.62 \times 10^{-12}$) in carcinoma tissues than in normal tissues. Also, it was obvious that methylation level of FBXO31 was elevated in carcinoma tissues relative to the normal tissues (Fig. 1C, $p < 1 \times 10^{-12}$). qRT-PCR analysis revealed that DNMT3B expression level in BC cell lines (MCF-7, MDA-MB-231, MDA-MB-453) was upregulated compared with that in MCF10A cells (Fig. 1D, $p < 0.001$). Among the three breast cancer cell lines (MCF-7, MDA-MB-231, MDA-MB-453), the expression level of DNMT3B was the highest in MCF-7 cells. Therefore, we chose the MCF-7 cells with the most significant expression in this model for further in-depth mechanism studies.

DNMT3B Silencing Inhibited the Viability, Migration and Invasion and Enhanced Apoptosis and FBXO31 Expression in MCF-7 Cells

To verify the specific effects of DNMT3B in BC cells, DNMT3B mRNA or protein expression was manipulated to be decreased in MCF-7 cells via successful transfection of Sh-DNMT3B (Fig. 2A–C, $p < 0.001$). Following the interference of Sh-DNMT3B in BC cells, we determined cell viability, apoptosis, migration, and invasion. As revealed in Fig. 2D–I, decrease of viability, migration, and invasion as well as increase of apoptosis in MCF-7 cells were detected in response to the silencing of DNMT3B ($p < 0.05$), suggesting that DNMT3B strengthened the malignant phenotypes of BC cells. Besides, we also measured apoptosis/proliferation-related protein expressions in Sh-DNMT3B-manipulated MCF-7 cells. In accordance with the results in Fig. 3A–E, Sh-DNMT3B upregulated Bax expression while downregulating Bcl-2, Ki67 and PCNA expressions in MCF-7 cells ($p < 0.001$), indicating that DNMT3B silencing suppressed malignant phenotypes of BC cells. Also, we evaluated the FBXO31 expression in Sh-DNMT3B-interfered MCF-7 cells. The results from Western blot and qRT-PCR analyses exhibited that FBXO31 mRNA/protein expression was enhanced after the silencing of DNMT3B (Fig. 3F–H, $p < 0.001$).

DNMT3B Silencing Diminished FBXO31 Methylation Level in MCF-7 Cells

The 5mC site of FBXO31 was predicted using RMBase database, and the results were presented in Fig. 4A. Thereafter, the FBXO31 methylation level in Sh-DNMT3B-manipulated MCF-7 cells was evaluated by MSP assay. Sh-DNMT3B diminished FBXO31 methylation level in MCF-7 cells (Fig. 4B,C, $p < 0.001$). These findings provided strong evidence that DNMT3B indeed

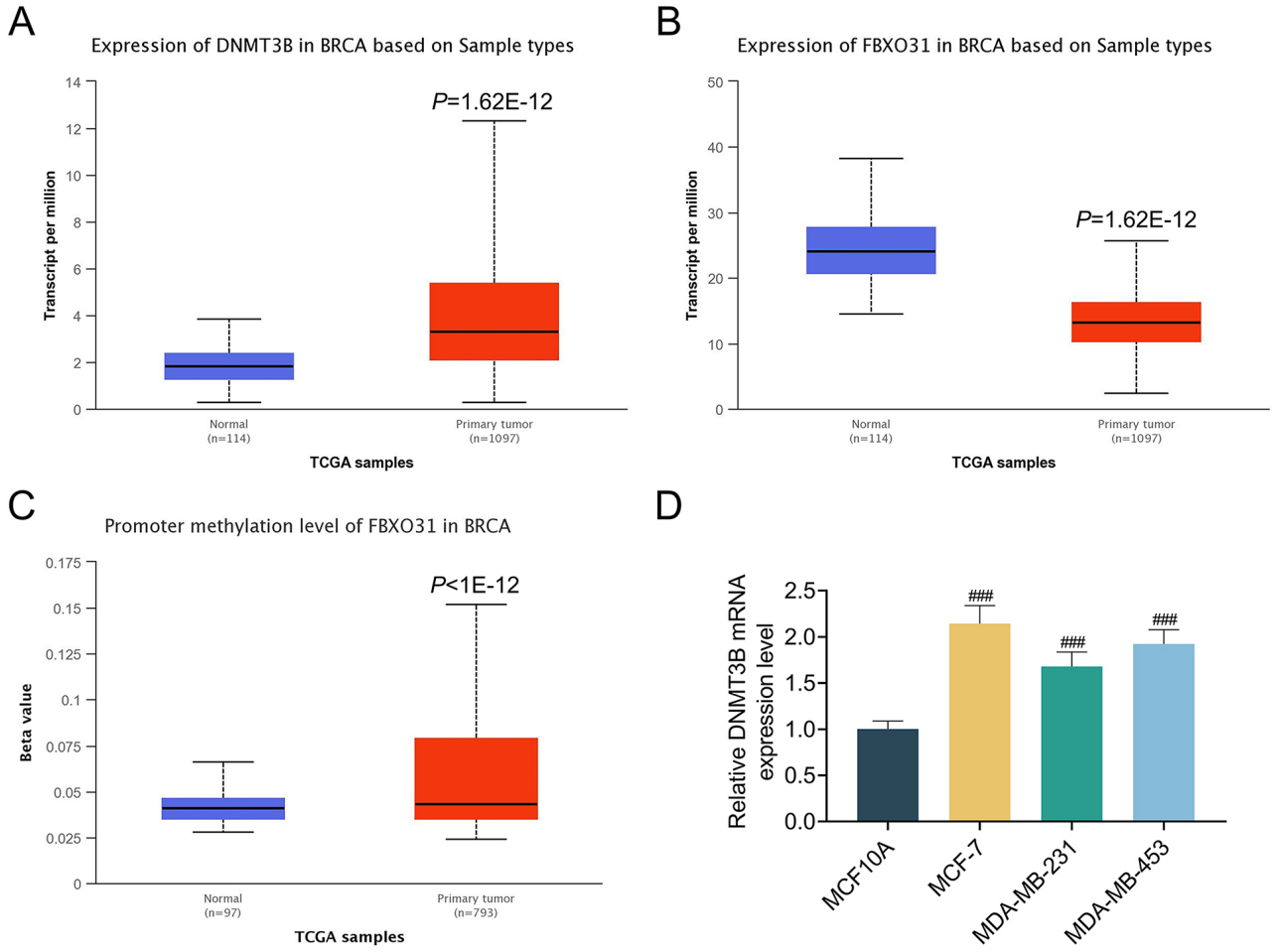

Fig. 1. DNMT3B level was upregulated while FBXO31 level was downregulated, and FBXO31 methylation level was elevated in BC. (A–C) The expression levels of DNMT3B and FBXO31 and methylation level of FBXO31 promoter in breast invasive carcinoma (BRCA) through UALCAN databases (https://ualcan.path.uab.edu/). (D) DNMT3B expression levels in BC cell lines (MCF-7, MDA-MB-231, MDA-MB-453) and human normal mammary epithelial cells (MCF10A) were tested by qRT-PCR. GAPDH was used as a loading control. n = 3. ###$p < 0.001$ vs. MCF10A. DNMT3B, DNA methyltransferase 3 beta; FBXO31, F-box protein 31; BC, breast cancer; UALCAN, University of Alabama at Birmingham Cancer Data Analysis Portal; qRT-PCR, quantitative real-time reverse transcription polymerase chain reaction; GAPDH, glyceraldehyde-3-phosphate dehydrogenase; TCGA, The Cancer Genome Atlas.

regulated FBXO31 expression through methylation modification. In addition, ChIP assay showed that the enrichment of FBXO31 promoter was higher in anti-DNMT3B group than that in anti-IgG group (Fig. 4D, $p < 0.001$), indicating that DNMT3B interacts with FBXO31.

DNMT3B Silencing Reversed the Effects of FBXO31 Silencing on the Viability, Apoptosis, Migration and Invasion of MCF-7 Cells

Further, we delved into regulatory relationship between DNMT3B and FBXO31 in BC cells. Accordingly, we transfected Sh-FBXO31 into MCF-7 cells to reduce FBXO31 expression, the success of which was proved by qRT-PCR (Fig. 5A, $p < 0.001$). The results in Fig. 5B,D,E revealed that FBXO31 silencing had no significant effect on DNMT3B expression, and DNMT3B expression was decreased in the Sh-DNMT3B+Sh-FBXO31 group ($p < 0.001$). The results in Fig. 5C,D,F revealed that FBXO31 level was elevated in MCF-7 cells transfected with Sh-DNMT3B and Sh-FBXO31 in comparison with that in Sh-FBXO31-interfered MCF-7 cells ($p < 0.01$), confirming that DNMT3B silencing promoted FBXO31 expression in BC cells.

The subsequent assays of MTT (Fig. 5G), flow cytometry (Fig. 5H,I), and Transwell assay (Fig. 6A–C) showed that Sh-FBXO31 promoted viability, migration, and invasion, but repressed apoptosis of MCF-7 cells ($p < 0.01$), which were all reversed following the interference of DNMT3B silencing ($p < 0.01$). Moreover, we additionally detected apoptosis/proliferation-associated protein expressions to further verify the regulation of DNMT3B and FBXO31 on malignant features of BC cells. According to

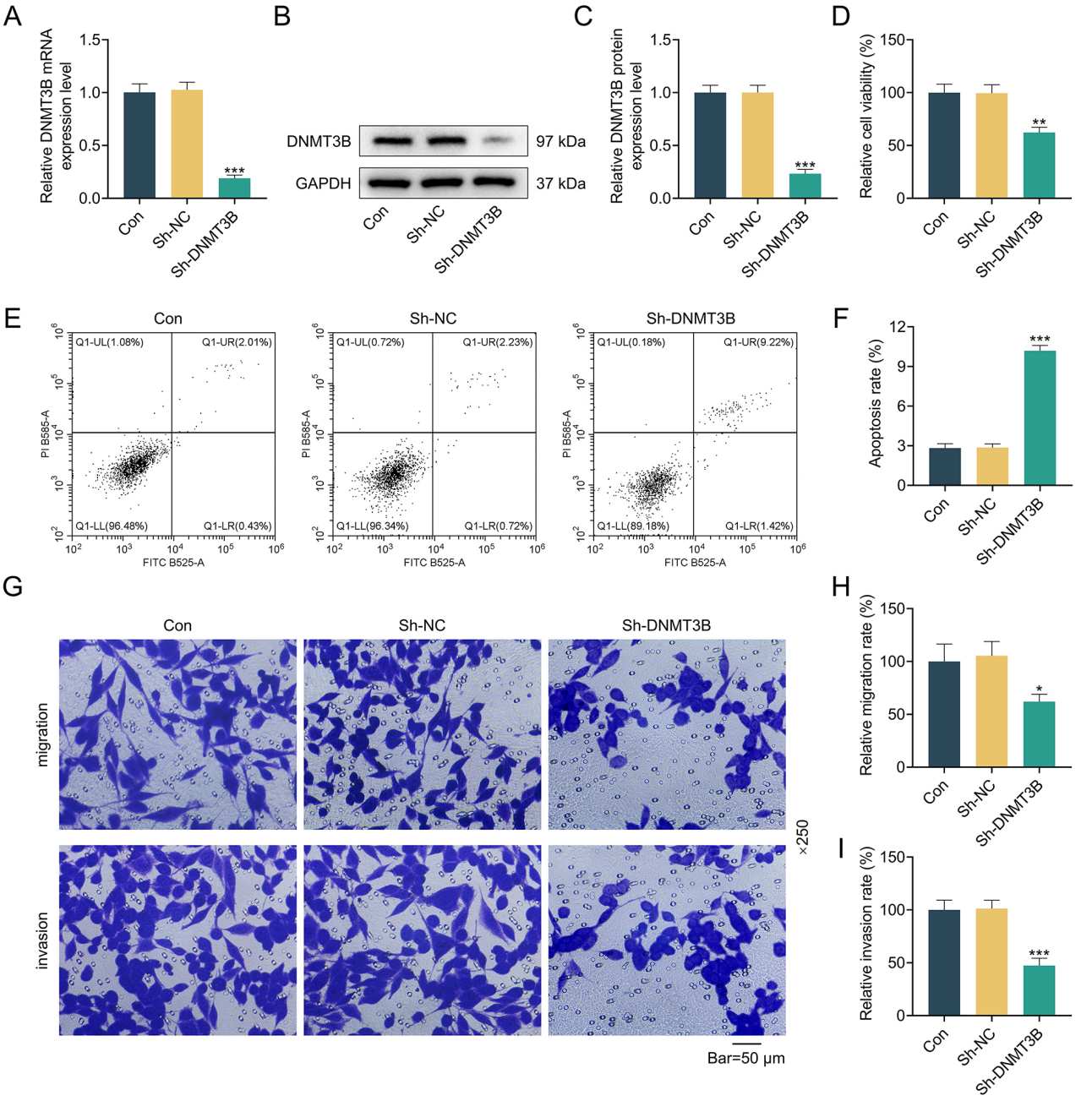

Fig. 2. DNMT3B silencing suppressed viability, invasion, and migration, but promoted apoptosis of MCF-7 cells. (A–C) DNMT3B mRNA or protein expression was manipulated to be decreased in MCF-7 cells via successful transfection of Sh-DNMT3B, which was verified by qRT-PCR analysis or Western blotting. GAPDH was used as a loading control. (D–I) Following the silencing of DNMT3B in MCF-7 cells, the cell viability was determined by MTT assay (D), apoptosis was tested through flow cytometry (E,F), and migration and invasion were measured by Transwell assay (G–I; scale: 50 μm; magnification: ×250). n = 3. *$p < 0.05$, **$p < 0.01$, ***$p < 0.001$ vs. Sh-NC. Sh-DNMT3B, short hairpin RNA against DNMT3B; MTT, 3-(4,5-dimethylthiazol-2-yl)-2,5-diphenyl-2H-tetrazolium bromide; Sh-NC, short hairpin RNA of negative control.

the results of Western blotting, Bax expression was reduced while Bcl-2, Ki67 and PCNA expressions in MCF-7 cells were elevated following the FBXO31 silencing (Fig. 6D–H, $p < 0.001$). The effects of FBXO31 silencing in MCF-7 cells were offset by further treatment with Sh-DNMT3B (Fig. 6D–H, $p < 0.001$).

Discussion

DNA methylation is vital in the regulation of gene transcription [28], and its aberrant patterns may serve as potential biomarkers in the diagnosis and treatment of cancers [29]. Notably, such alterations have been identified

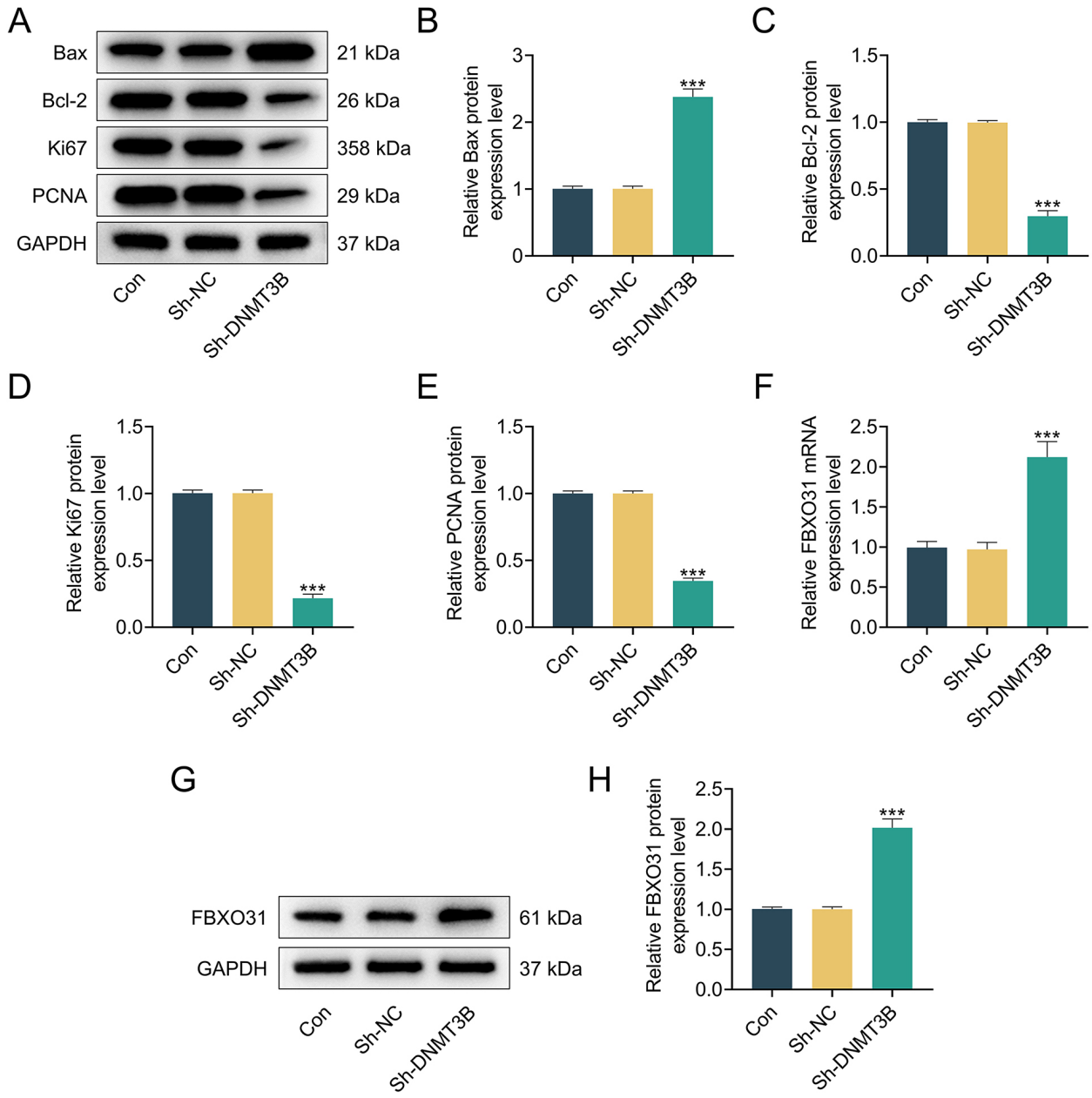

Fig. 3. DNMT3B silencing promoted apoptosis while suppressing proliferation of MCF-7 cells. (A–E) Apoptosis/proliferation-related protein expressions were measured in MCF-7 cells following the silencing of DNMT3B. GAPDH was used as a loading control. (F–H) FBXO31 expression in Sh-DNMT3B-interfered MCF-7 cells was detected by qRT-PCR analysis or Western blotting. GAPDH was used as a loading control. n = 3. ***$p < 0.001$ vs. Sh-NC. FBXO31, F-box protein 31; Bax, BCL2 associated X; Bcl-2, B cell leukemia/lymphoma 2; PCNA, proliferating cell nuclear antigen.

in BC [30]; however, the underlying molecular mechanism remain insufficiently. In this study, bioinformatic analyses revealed downregulation of FBXO31 in BC and its upregulated methylation, alongside enhanced DNMT3B expression in BC. On this basis, we performed *in-vitro* experiments to explore the specific roles of DNMT3B and FBXO31 in MCF-7 cells (Luminal A subtype). This study demonstrated that silencing DNMT3B inhibited malignant phenotypes in MCF-7 cells, an effect associated with reduced FBXO31 methylation and increased FBXO31 expression. These findings indicate that DNMT3B may promote tumor progression by mediating epigenetic silencing FBXO31 through DNA methylation.

As a DNA methyltransferase, DNMT3B is responsible for the regulation of DNA methylation [19]. Present research has clarified the function of DNMT3B in dif-

A

ModID	m5C_site_277
Chromosome	chr16
ModStart	87417652
ModEnd	87417653
Strand	-
ModType	m5C
FullName	5-methylcytidine
ModName	tRNA-Met|N|m5C|hTrm4
SupportNum	1
SupportList	GSE38957
GeneName	FBXO31,FBXO31,tRNA-Met_,chr16.tRNA22-MetCAT
GeneType	processed_transcript,protein_coding,tRNA,tRNA
Region	intron,intron,exon,exon
Sequence	CAGTCTCATAATCTGAAGGTCGTGAGTTCGAGCCTCACACG
PubMed ID	23604283

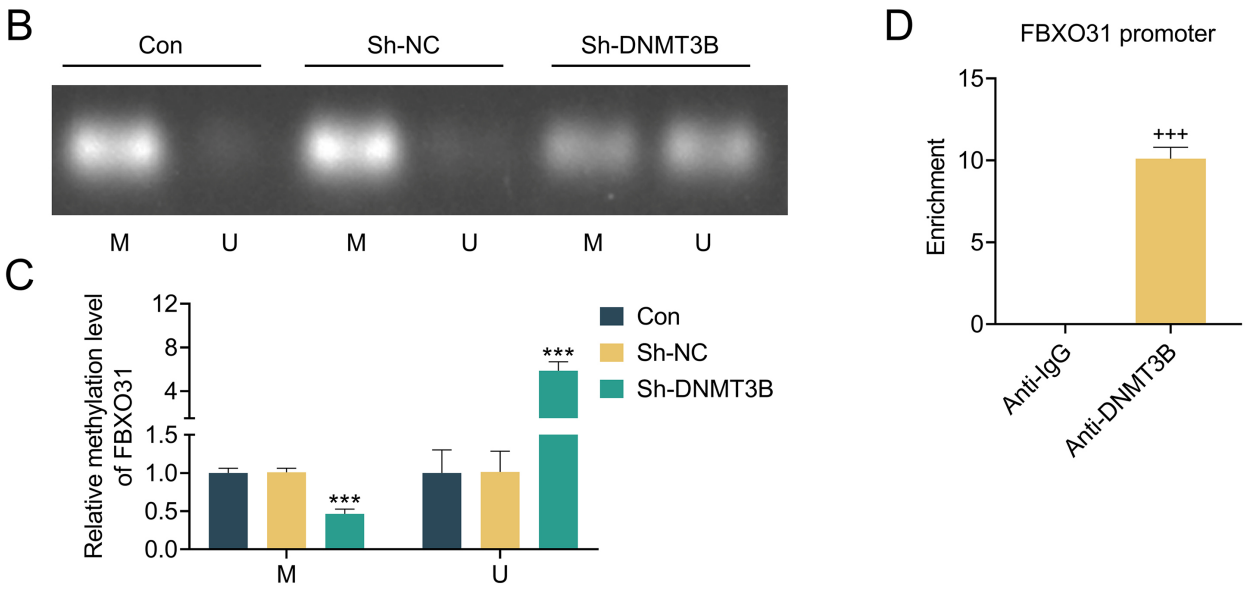

Fig. 4. DNMT3B silencing diminished FBXO31 methylation level in MCF-7 cells. (A) The 5mC site of FBXO31 was predicted using RMBase database (https://rna.sysu.edu.cn/rmbase/index.php). (B,C) FBXO31 methylation level in Sh-DNMT3B-transfected MCF-7 cells was evaluated by MSP assay. (D) The binding between DNMT3B and FBXO31 promoters in MCF-7 cells. 5mC, 5-methylcytosine; MSP, methylation-specific polymerase chain reaction; M, methylated; U, unmethylated. ***$p < 0.001$ vs. Sh-NC; +++$p < 0.001$ vs. Anti-IgG.

ferent cancers, including esophageal cancer [31], thyroid cancer [32], and colorectal cancer [33]. Upregulation of DNMT3B participates in the modulation of malignant phenotype of colorectal cancer [34]. Similarly, DNMT3B has been proven to regulate PCDH17 via methylation to affect the malignant behaviors of hepatocellular carcinoma [35]. DNMT3B, as one of the 5mC regulators, is highly expressed in BC and associated with dismal prognosis of BC patients [22]. Intriguingly, DNMT3B can be recruited by RAMP2-AS1 to the C-X-C Motif Chemokine Ligand 11 (CXCL11) promoter region to regulate CXCL11 methylation and thus suppress the malignant phenotype of BC [36]. These findings prompted us to investigate whether DNMT3B can have an impact on malignant phenotype of BC through mediating the methylation levels of some novel genes. In the present study, we firstly confirmed that viability, migration, and invasion of BC cells were suppressed while the apoptosis was enhanced following the knockdown of DNMT3B, which indicated that DNMT3B silencing suppressed malignant phenotype of BC cells. To fur-

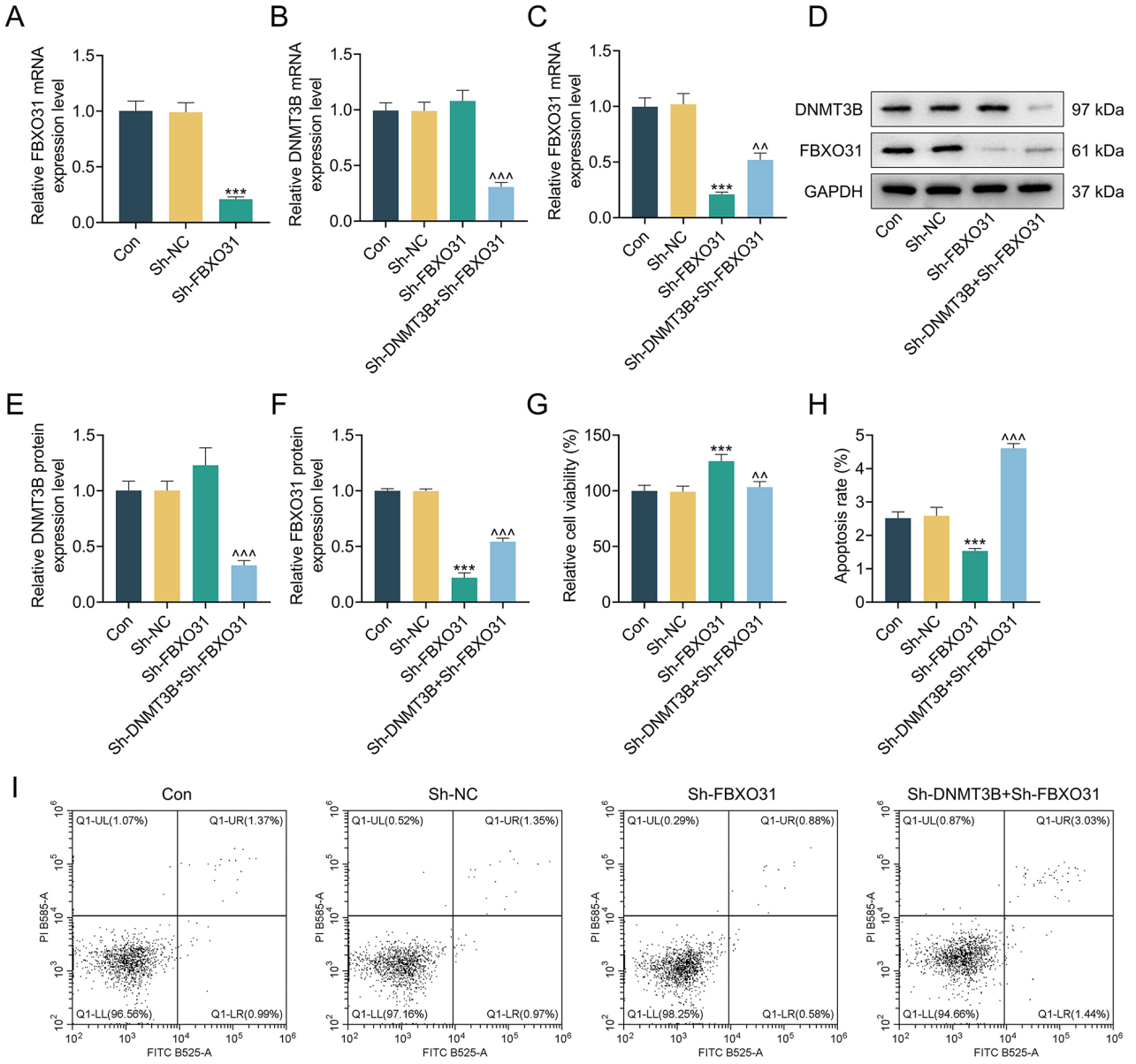

Fig. 5. DNMT3B silencing reversed the effects of FBXO31 silencing on viability and apoptosis of MCF-7 cells. (A) Sh-FBXO31 was transfected into MCF-7 cells to reduce FBXO31 expression, which was proved to be successful by qRT-PCR analysis. GAPDH was used as a loading control. (B–F) Following the silencing of DNMT3B and FBXO31 in MCF-7 cells, DNMT3B and FBXO31 mRNA expression levels were measured through qRT-PCR analysis (B,C), and their protein expression levels were analyzed by Western blotting, with GAPDH as a loading control (D–F). (G–I) Following the silencing of DNMT3B and FBXO31 in MCF-7 cells, the cell viability was determined by MTT assay (G), and apoptosis was tested through flow cytometry (H,I). n = 3. ***$p < 0.001$ vs. Sh-NC; ^^$p < 0.01$, ^^^$p < 0.001$ vs. Sh-FBXO31.

ther validate these observations, we examined the expression of key apoptosis and proliferation markers. Bax is a proapoptotic protein while Bcl-2 is an anti-apoptotic protein [37]. Ki67 and PCNA are considered as the proliferation-related markers for the diagnosis of BC [38]. These findings demonstrate that DNMT3B silencing attenuates the malignant phenotype of Luminal A subtype BC cells by enhancing apoptosis and reducing proliferation, migration, and invasion.

Furthermore, we delved into the downstream genes of DNMT3B in MCF-7 cells and the function of FBXO31 in BC. FBXO31 has garnered increasing attention in recent years due to its involvement in BC. FBXO31 has been demonstrated to be downregulated in BC and serves as a tumor-inhibitory gene, regulating proliferation and migration in BC [25]. Consistent with these findings, our preliminary bioinformatics also revealed that the expression of FBXO31 was reduced in BC and its methylation

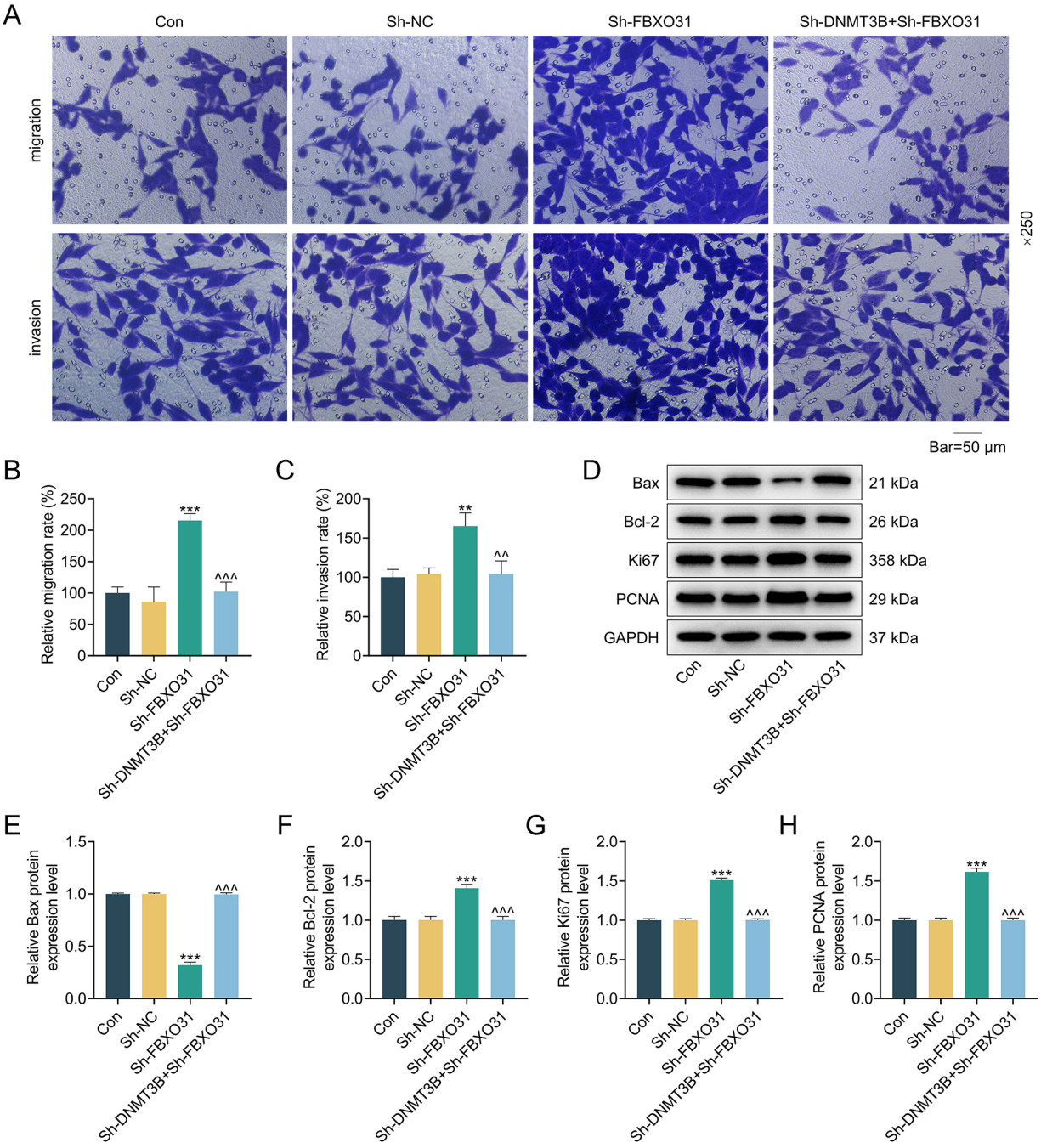

Fig. 6. DNMT3B silencing offset the effects of FBXO31 silencing on migration, invasion, apoptosis, and proliferation in MCF-7 cells. (A–H) Following the silencing of DNMT3B and FBXO31 in MCF-7 cells, migration and invasion were measured by Transwell assay (A–C; scale: 50 μm; magnification: ×250), and apoptosis/proliferation-related protein expressions were tested by Western blotting (D–H). GAPDH was used as a loading control. n = 3. $^{**}p < 0.01$, $^{***}p < 0.001$ vs. Sh-NC; $^{\wedge\wedge}p < 0.01$, $^{\wedge\wedge\wedge}p < 0.001$ vs. Sh-FBXO31.

level was upregulated. However, the mechanism underlying FBXO31 methylation and its regulation by DNMT3B in BC remain poorly understood. In the present study, the presence of a 5mC site in FBXO31 was firstly confirmed by bioinformatics, denoting that DNMT3B may regulate FBXO31 via methylation modifications to affect the malignant phenotype of BC. Subsequently experimental validation demonstrated that FBXO31 methylation level was reduced following the knockdown of DNMT3B and restored its expression in MCF-7 cells. These data suggested that DNMT3B can downregulate FBXO31 expression via promoting FBXO31 methylation. On the other hand, we confirmed the promoted malignant phenotype of BC following the silencing of FBXO31, suggesting that FBXO31 played

a negative role in the progression of BC. In addition, the effects of FBXO31 silencing on MCF-7 cells were all offset by DNMT3B deletion, indicating the regulatory relationship of DNMT3B and FBXO31. Accordingly, we preliminarily concluded that DNMT3B silencing upregulated FBXO31 expression via reducing its methylation level, and inhibited the malignant phenotype of MCF-7 cells.

Nevertheless, this study has several limitations. First, this research is limited to MCF-7 cells (Luminal A subtype), while BC exhibits significant molecular heterogeneity, and the regulatory mechanisms of this pathway in other subtypes (such as Luminal B, HER2 positive, and triple-negative BC) have not been pinpointed. Future research needs to comprehensively verify the function of the DNMT3B and FBXO31 in BC cell models of different molecular subtypes. Second, the current research findings mainly are based largely on *in vitro* cell experiments, lacking validation from clinical samples (such as tissue expression profiles, methylation status and correlation analysis with clinical pathological characteristics) and validation in animal models. Future studies integrating clinical sample analysis and animal experiments will be essential to comprehensively evaluate the biological significance and potential translational value of this pathway. Third, the upstream regulators and downstream effectors of DNMT3B in this context remain incompletely characterized, which warrants further elucidation.

Conclusions

In conclusion, our study confirms the regulation of DNMT3B on FBXO31 methylation in BC. Collectively, DNMT3B silencing alleviates malignant phenotypes of Luminal A BC cells by suppressing FBXO31 methylation, which paves the way for the potential therapeutic strategies in Luminal A BC.

Availability of Data and Materials

The analyzed data sets generated during the study are available from the corresponding author on reasonable request.

Author Contributions

Substantial contributions to conception and design: JL; Data acquisition, data analysis and interpretation: SH, ZZ, LC and YW; Drafting the article or critically revising it for important intellectual content: YW; Critical revision of the manuscript for important intellectual content: All authors. Final approval of the version to be published: All authors; Agreement to be accountable for all aspects of the work in ensuring that questions related to the accuracy or integrity of the work are appropriately investigated and resolved: All authors.

Ethics Approval and Consent to Participate

Not applicable.

Acknowledgment

Not applicable.

Funding

This work was supported by Natural Science Foundation of Hunan Province (No. 2021JJ31027).

Conflict of Interest

The authors declare no conflict of interest.

References

[1] Siegel RL, Miller KD, Wagle NS, Jemal A. Cancer statistics, 2023. CA: A Cancer Journal for Clinicians. 2023; 73: 17–48. https://doi.org/10.3322/caac.21763.

[2] Feng R, Su Q, Huang X, Basnet T, Xu X, Ye W. Cancer situation in China: what does the China cancer map indicate from the first national death survey to the latest cancer registration? Cancer Communications. 2023; 43: 75–86. https://doi.org/10.1002/cac2.12393.

[3] Picon-Ruiz M, Morata-Tarifa C, Valle-Goffin JJ, Friedman ER, Slingerland JM. Obesity and adverse breast cancer risk and outcome: Mechanistic insights and strategies for intervention. CA: A Cancer Journal for Clinicians. 2017; 67: 378–397. https://doi.org/10.3322/caac.21405.

[4] Burstein HJ, Curigliano G, Thürlimann B, Weber WP, Poortmans P, Regan MM, *et al*. Customizing local and systemic therapies for women with early breast cancer: the St. Gallen International Consensus Guidelines for treatment of early breast cancer 2021. Annals of Oncology. 2021; 32: 1216–1235. https://doi.org/10.1016/j.annonc.2021.06.023.

[5] Ribeiro R, Carvalho MJ, Goncalves J, Moreira JN. Immunotherapy in triple-negative breast cancer: Insights into tumor immune landscape and therapeutic opportunities. Frontiers in Molecular Biosciences. 2022; 9: 903065. https://doi.org/10.3389/fmolb.2022.903065.

[6] Zhong W, Zhong G, Ye W, Jin X. Assessing Surgical Benefits and Creating a Prognostic Model for Breast Cancer with Lung-only Metastasis: An Analysis of the National Cancer Database. Annali Italiani Di Chirurgia. 2024; 95: 391–400. https://doi.org/10.62713/aic.3365.

[7] Zhu SY, Yu KD. Breast Cancer Vaccines: Disappointing or Promising? Frontiers in Immunology. 2022; 13: 828386. https://doi.org/10.3389/fimmu.2022.828386.

[8] Blucher AS, Mills GB, Tsang YH. Precision oncology for breast cancer through clinical trials. Clinical & Experimental Metastasis. 2022; 39: 71–78. https://doi.org/10.1007/s10585-021-10092-0.

[9] Klutstein M, Nejman D, Greenfield R, Cedar H. DNA Methylation in Cancer and Aging. Cancer Research. 2016; 76: 3446–3450. https://doi.org/10.1158/0008-5472.CAN-15-3278.

[10] Dmitrijeva M, Ossowski S, Serrano L, Schaefer MH. Tissue-specific DNA methylation loss during ageing and carcinogenesis is linked to chromosome structure, replication timing and cell division rates. Nucleic Acids Research. 2018; 46: 7022–7039. https://doi.org/10.1093/nar/gky498.

[11] Ye P, Luan Y, Chen K, Liu Y, Xiao C, Xie Z. MethSMRT:

an integrative database for DNA N6-methyladenine and N4-methylcytosine generated by single-molecular real-time sequencing. Nucleic Acids Research. 2017; 45: D85–D89. https://doi.org/10.1093/nar/gkw950.

[12] Lv H, Dao FY, Zhang D, Yang H, Lin H. Advances in mapping the epigenetic modifications of 5-methylcytosine (5mC), N6-methyladenine (6mA), and N4-methylcytosine (4mC). Biotechnology and Bioengineering. 2021; 118: 4204–4216. https://doi.org/10.1002/bit.27911.

[13] Pfeifer GP. Defining Driver DNA Methylation Changes in Human Cancer. International Journal of Molecular Sciences. 2018; 19: 1166. https://doi.org/10.3390/ijms19041166.

[14] Gagliardi M, Strazzullo M, Matarazzo MR. DNMT3B Functions: Novel Insights From Human Disease. Frontiers in Cell and Developmental Biology. 2018; 6: 140. https://doi.org/10.3389/fcell.2018.00140.

[15] Győrffy B, Bottai G, Fleischer T, Munkácsy G, Budczies J, Paladini L, *et al*. Aberrant DNA methylation impacts gene expression and prognosis in breast cancer subtypes. International Journal of Cancer. 2016; 138: 87–97. https://doi.org/10.1002/ijc.29684.

[16] Li Z, Heng J, Yan J, Guo X, Tang L, Chen M, *et al*. Integrated analysis of gene expression and methylation profiles of 48 candidate genes in breast cancer patients. Breast Cancer Research and Treatment. 2016; 160: 371–383. https://doi.org/10.1007/s10549-016-4004-8.

[17] Janostiak R, Vyas M, Cicek AF, Wajapeyee N, Harigopal M. Loss of c-KIT expression in breast cancer correlates with malignant transformation of breast epithelium and is mediated by KIT gene promoter DNA hypermethylation. Experimental and Molecular Pathology. 2018; 105: 41–49. https://doi.org/10.1016/j.yexmp.2018.05.011.

[18] Naghitorabi M, Mohammadi Asl J, Mir Mohammad Sadeghi H, Rabbani M, Jafarian-Dehkordi A, Javanmard HS. Quantitative evaluation of DNMT3B promoter methylation in breast cancer patients using differential high resolution melting analysis. Research in Pharmaceutical Sciences. 2013; 8: 167–175.

[19] Man X, Li Q, Wang B, Zhang H, Zhang S, Li Z. DNMT3A and DNMT3B in Breast Tumorigenesis and Potential Therapy. Frontiers in Cell and Developmental Biology. 2022; 10: 916725. https://doi.org/10.3389/fcell.2022.916725.

[20] Tavakolian S, Goudarzi H, Faghihloo E. E-cadherin, Snail, ZEB-1, DNMT1, DNMT3A and DNMT3B expression in normal and breast cancer tissues. Acta Biochimica Polonica. 2019; 66: 409–414. https://doi.org/10.18388/abp.2019_2808.

[21] Roscigno G, Quintavalle C, Donnarumma E, Puoti I, Diaz-Lagares A, Iaboni M, *et al*. MiR-221 promotes stemness of breast cancer cells by targeting DNMT3b. Oncotarget. 2016; 7: 580–592. https://doi.org/10.18632/oncotarget.5979.

[22] Liu J, Xiao S, Chen J, Lou W, Chen X. A Comprehensive Analysis for Expression, Diagnosis, and Prognosis of m^5C Regulator in Breast Cancer and Its ncRNA-mRNA Regulatory Mechanism. Frontiers in Genetics. 2022; 13: 822721. https://doi.org/10.3389/fgene.2022.822721.

[23] Zhang W, Zhi Y, Wu Z, Chen Y, Feng L, He J, *et al*. ZBTB12 promotes breast cancer progression through transcriptional activation of the DNMT3B/ALDH1A2 axis. Biochemical and Biophysical Research Communications. 2025; 776: 152214. https://doi.org/10.1016/j.bbrc.2025.152214.

[24] Huang ZF, Tang YL, Shen ZL, Yang KY, Gao K. UXT, a novel DNMT3b-binding protein, promotes breast cancer progression via negatively modulating lncRNA MEG3/p53 axis. Molecular Therapy Oncolytics. 2021; 24: 497–506. https://doi.org/10.1016/j.omto.2021.12.008.

[25] Liu D, Xia H, Wang F, Chen C, Long J. MicroRNA-210 interacts with FBXO31 to regulate cancer proliferation cell cycle and migration in human breast cancer. OncoTargets and Therapy. 2016; 9: 5245–5255. https://doi.org/10.2147/OTT.S110969.

[26] Kumar R, Neilsen PM, Crawford J, McKirdy R, Lee J, Powell JA, *et al*. FBXO31 is the chromosome 16q24.3 senescence gene, a candidate breast tumor suppressor, and a component of an SCF complex. Cancer Research. 2005; 65: 11304–11313. https://doi.org/10.1158/0008-5472.CAN-05-0936.

[27] Livak KJ, Schmittgen TD. Analysis of relative gene expression data using real-time quantitative PCR and the 2(-Delta Delta C(T)) Method. Methods. 2001; 25: 402–408. https://doi.org/10.1006/meth.2001.1262.

[28] Sun Z, Wang Y, Song Z, Zhang H, Wang Y, Liu K, *et al*. DNA methylation in transposable elements buffers the connection between three-dimensional chromatin organization and gene transcription upon rice genome duplication. Journal of Advanced Research. 2022; 42: 41–53. https://doi.org/10.1016/j.jare.2022.07.007.

[29] Ding W, Chen G, Shi T. Integrative analysis identifies potential DNA methylation biomarkers for pan-cancer diagnosis and prognosis. Epigenetics. 2019; 14: 67–80. https://doi.org/10.1080/15592294.2019.1568178.

[30] Mahmoud AM, Ali MM. Methyl Donor Micronutrients that Modify DNA Methylation and Cancer Outcome. Nutrients. 2019; 11: 608. https://doi.org/10.3390/nu11030608.

[31] Zhou W, Zhu H, Xu Y, Gu L, Wu W, Zhang Y, *et al*. miR-498/DNMT3b Axis Mediates Resistance to Radiotherapy in Esophageal Cancer Cells. Cancer Biotherapy & Radiopharmaceuticals. 2022; 37: 287–299. https://doi.org/10.1089/cbr.2020.4227.

[32] Zhu X, Xue C, Kang X, Jia X, Wang L, Younis MH, *et al*. DNMT3B-mediated FAM111B methylation promotes papillary thyroid tumor glycolysis, growth and metastasis. International Journal of Biological Sciences. 2022; 18: 4372–4387. https://doi.org/10.7150/ijbs.72397.

[33] Zhou L, Pan LZ, Fan YJ. DNMT3b affects colorectal cancer development by regulating FLI1 through DNA hypermethylation. The Kaohsiung Journal of Medical Sciences. 2023; 39: 364–376. https://doi.org/10.1002/kjm2.12647.

[34] Zou L, Zhan N, Wu H, Huang B, Cui D, Chai H. Circ_0000467 modulates malignant characteristics of colorectal cancer via sponging miR-651-5p and up-regulating DNMT3B. Nucleosides, Nucleotides & Nucleic Acids. 2023; 42: 134–150. https://doi.org/10.1080/15257770.2022.2112050.

[35] Liu Y, Zhang Y, Du D, Gu X, Zhou S. PCDH17 is regulated by methylation of DNMT3B and affects the malignant biological behavior of HCC through EMT. Experimental Cell Research. 2022; 418: 113245. https://doi.org/10.1016/j.yexcr.2022.113245.

[36] Li L, Gan YP, Peng H. RAMP2-AS1 inhibits CXCL11 expression to suppress malignant phenotype of breast cancer by recruiting DNMT1 and DNMT3B. Experimental Cell Research. 2022; 416: 113139. https://doi.org/10.1016/j.yexcr.2022.113139.

[37] Klimentova EA, Suchkov IA, Shchulkin AV, Glazkova AP, Kalinin RE. Expression of Apoptotic Markers Bcl-2 and Bax in the Vascular Wall. Sovremennye Tekhnologii V Meditsine. 2021; 13: 46–50. https://doi.org/10.17691/stm2021.13.2.05.

[38] Juríková M, Danihel Ľ, Polák Š, Varga I. Ki67, PCNA, and MCM proteins: Markers of proliferation in the diagnosis of breast cancer. Acta Histochemica. 2016; 118: 544–552. https://doi.org/10.1016/j.acthis.2016.05.002.